

## A REVIEW OF SELECTED CONTRIBUTIONS TO HARMONIC GENERATION AND RADIATION DAMAGE RESEARCH BY OTTO BUCK

D. O. Thompson  
Center for Nondestructive Evaluation and  
Department of Aerospace Engineering and Engineering Mechanics  
Iowa State University  
1915 Scholl Road  
Ames, IA 50011

### INTRODUCTION

Otto Buck was an excellent scientist and a close personal friend. I first met Otto at the newly founded North American Aviation Science Center which I joined in April, 1964, after leaving the Oak Ridge National Laboratory. Otto joined a week later from the Max Planck Institute in Stuttgart, Germany. We were assigned to work together, thus beginning a wonderful experience that lasted up to his passing in November, 1997. In our collaborations, Otto emphasized the theoretical modeling aspects of the work while I emphasized the experimental. The purpose of this paper is to recall in memoriam some of the highlights of Otto's early contributions to the scientific literature resulting from our collaboration. The period covered extends approximately from 1964 to 1974. Previous to this time, Otto had made significant contributions to several areas in metal physics including elasticity, radiation damage, and plastic deformation studies [1-8]. Because of the memorial nature of the paper, an attempt will be made to show highlights of Otto's developments only and not to emphasize the individual details and rigor that always characterized Otto's work. The reader is referred to the original publications to extract those.

### Technical Highlights

Three topics will be discussed here that resulted from our collaborations; they are: the relation of finite amplitude waves to third order elastic constants (TOEC), the nature of reflections from stress-free boundaries of harmonic waves generated by finite amplitude waves, and descriptions of point defect/dislocation interactions derived from low amplitude internal function studies. A limited effort will be made to say a few words about interests that motivated the work at the time that it was done, the specific problem addressed and the approaches taken, and highlights of results obtained.

## Determination of Third Order Elastic Constants From Finite Amplitude Ultrasonic Waves

There was significant motivation to pursue new ways to measure third order constants at the time this work was undertaken [9]. On the one hand, a number of authors were in pursuit of an understanding of the non-linear nature of interatomic forces in solids. Examples are given in [10,11]. This interest was further enhanced by new capabilities [12-15] reported for the generation of harmonics by finite amplitude ultrasonic waves, a phenomenon clearly related to the nature of non-linear interatomic forces and the third order constants. This was exciting, for this approach offered new opportunities for the measurement of the third order constants in non-transparent solids without the application of external stresses. Thus, this difficult and timely study aimed at the development of relationships between the second harmonic wave amplitudes generated by a fundamental finite amplitude ultrasonic wave and the third order elastic constants of the material was undertaken. Because of the mathematical complexities of the problem, the work focused on the development of such relationships in cubic materials with wave propagation in arbitrary directions within a {110} type crystal plane using both longitudinal and transverse ultrasonic waves. Careful attention was paid to the utilization of model geometries that were compatible with usual ultrasonic experimental procedures.

A fairly general approach was taken in setting up the problem. The equation of motion was written in Lagrangian coordinates as

$$\rho \ddot{\underline{u}} = \text{div}_x \underline{\sigma} \quad (1)$$

in which  $\gamma$  is the material density,  $\ddot{\underline{u}}$  the vector acceleration of the unit cell, and  $\underline{\sigma}$  the stress tensor given by

$$\underline{\sigma} = \frac{\rho}{\rho_o} J \frac{\partial W}{\partial \underline{\gamma}} \underline{\tilde{J}}. \quad (2)$$

In (2),  $\rho_o$  is the static density,  $J$  and  $\tilde{J}$  are the Jacobian and its inverse,  $\gamma_{ik}$  is defined by

$$\gamma_{ik} = \frac{1}{2} \sum_l \left( \frac{\partial x_l}{\partial a_i} \frac{\partial x_l}{\partial a_k} - \delta_{ik} \right), \quad (3)$$

in which the  $a$ 's are the unit cell axes, and  $W$  is the energy density and includes cubic terms in the strain; it introduces the third order elastic constants into the computation.

Solutions were obtained for the equation of motion using a standard perturbation technique. The total particle displacement vector  $\underline{u}$  was expanded in a power series and both the infinitely small wave amplitude and the second order harmonic amplitudes that contain information on the third order constants were obtained.

Neglecting here any discussion of the usual first order, infinitely small amplitude solutions, it was found that the second order, harmonic waves that contain the third order constants were generally very complex and contained dependencies upon both the fundamental and harmonic frequencies as well as amplitude terms that depend both linearly and quadratically upon the generating frequency and the path length of the propagating wave. For example, second order displacements  $u^{**}$  generated by a compressional excitation of amplitude  $A$  or a transverse excitation of amplitude  $B$  could be written as

$$u^{**}(A) = \begin{pmatrix} O \\ B_1 \\ A_1 \end{pmatrix} \omega^2 s \cos \left[ 2\omega t - \frac{2\omega}{v_1} s \right] + \begin{pmatrix} O \\ O \\ A_2 \end{pmatrix} \omega s \sin \left[ 2\omega t - \frac{2\omega}{v_1} s \right], \quad (4)$$

and

$$u_2^{**}(B) = \begin{pmatrix} O \\ B_1 \\ A_1 \end{pmatrix} \omega^2 s \cos \left[ 2\omega t - \frac{2\omega}{v_2} s \right] + \begin{pmatrix} O \\ O \\ A_2 \end{pmatrix} \omega s \sin \left[ 2\omega t - \frac{2\omega}{v_2} s \right]. \quad (5)$$

In Equation (4), the harmonic displacement  $u^{**}$  due to an initial compressional excitation  $A$  has, in general, both shear ( $B_1$ ) and longitudinal ( $A_1$ ) components proportional to  $\omega^2$  and  $s$ , the distance the wave has propagated, and a longitudinal component ( $A_2$ ) proportional only to  $\omega$  and independent of distance propagated. The harmonic displacement  $u_2^{**}$  generated by an initial transverse impulse  $B$  has a similar structure.

In order to get results useful to the determination of the third order elastic constants, computations were made for specific propagation directions within the  $\{110\}$  type plane. Table I shows results obtained in which the coefficients of the harmonic displacement amplitudes are expressed in terms of the third order constants for longitudinal waves. Table II shows the same results for transverse waves polarized within the  $\{110\}$  type plane.

Otto's work in the development of theoretical relationships for coupling the third order elastic constants to the harmonic amplitudes generated by finite amplitude ultrasonic excitations has several important consequences. He determined that it would be possible to determine  $C_{111}$ ,  $C_{112}$ ,  $C_{166}$  and  $C_{144} + C_{456}$  by usual ultrasonic measurement techniques using various crystalline orientations. He also showed that this method of determination of the third order constants is not affected by values of fourth and higher order elastic constants since these constants do not contribute to the second harmonic generation. Finally, the work is obviously fundamental to current activities in NDE in the use of the so-called non-linear parameter for materials characterization.

#### Reflections of Harmonic Generation by Finite Amplitude Waves at Stress-Free Boundaries

In order to have confidence in the utilization of standard ultrasonic pulse echo techniques for the measurement of third order constants and attenuation effects, there was a strong need to develop and validate models that describe the reflections of distorted finite amplitude waves at stress-free boundaries, the key technique for ultrasonic measurements. Since it was shown in Equation (4) that the second harmonic of the distorted finite amplitude wave grew linearly with the distance traveled (neglecting attenuation effects), it was not completely obvious as to how the harmonic would behave under reflection—whether it would continue to grow undisturbed or follow some other behavior. Thus, strong motivation existed to increase our understanding of the behavior of reflection phenomenon of stress-free boundaries.

A combined theoretical and experimental approach was developed. Theoretically, the model-based studies assumed that the stress components of the fundamental and harmonic components of the distorted propagating wave vanish independently at the stress-free boundary [9]. In order to satisfy this condition, it was determined that, in addition to

the incident and reflected waves being present at the boundary, it was necessary to assume that an additional wave was generated at the boundary. Thus, solutions for the harmonic displacement at a stress-free boundary were found to have the form

$$u_{1\text{ total}}'' = u_{1\text{ incident}}'' + u_{1\text{ reflected}}'' + u_{1\text{ added}}'' \quad (6)$$

For a compressional wave propagating in a [001], [111], or [110] direction in a {110} type plane at the boundary, Equation (6) becomes

$$\begin{aligned} u_1''(A)_{TOTAL} = & A_1 \omega^2 s \left\{ \cos \left[ 2\omega t - \frac{2\omega s}{v_1} \right] + \cos \left[ 2\omega t - \frac{2\omega}{v_1} (2L - S) \right] \right\} \\ & - A_2 \omega v_1 \sin \left\{ 2\omega t - \frac{2\omega}{v_1} (2L - s) \right\} - 2A_1 \omega v_1 \sin \frac{2\omega}{v_1} (L - s) \\ & + 4A_1 \omega^2 (L - L_{\text{interaction}} - s). \end{aligned} \quad (7)$$

Here,  $L$  is the length of the sample,  $s$  is the propagation distance, and  $v_1$  is the acoustic compressional wave speed. Contributions from the wave generated at the boundary are interesting, for they introduce a time independent length expansion term that depends upon the square of the frequency and parameters involving the length of the sample  $L$ , the distance  $s$  that the wave has propagated, and an interaction length that is related to the pulse length. The reader is referred to the original work for details.

The analysis that Otto developed allowed several important conclusions to be developed for reflection of finite waves at stress-free boundaries. In the absence of attenuation, they were:

- the amplitude of the harmonic increases with path length up to the boundary; after reflection, the harmonic amplitude decreases becoming zero again on the original.
- the cycle repeats itself for each round trip; hence, standard pulse echo techniques can be used for measurement of attenuation.
- attenuation of the harmonics should be twice that of the fundamental.
- a time independent extension of the sample occurs in the interaction zone where incident and reflected waves interact.

Several pieces of experimental work were undertaken in order to verify these conclusions. They included an experimental paper [16] that describes results with fused silica samples and the development of an ultrasonic spectrometer [17]. Figure 1 shows the multiple harmonics that could be detected with the capacity-microphone spectrometer approach and Fig. 2 shows measured results for the reflection of both the fundamental (25 MHz) and harmonic (50 MHz) in the fused silica. The results show that the harmonic echoes behave as predicted, and that the measured attenuation for the harmonic was 0.30 dB/cm, just twice the 0.15 dB/cm observed for the fundamental.

#### Point Defect/Dislocation Interactions

A third topic to which Otto and his colleagues contributed significantly dealt with the development of an understanding of the interactions between point defects, i.e., vacancies and interstitials, and dislocations. This interest was motivated both by an active

Table I. Harmonic amplitudes and third order elastic constants - Longitudinal waves.

Terms in $\omega^2 s$	
Propagation Direction	Results
[001]	$A_1 = \frac{3}{8} \frac{\rho_o}{C_{11}} \left( 1 + 2 \frac{C_{111}}{C_{11}} \right) A_o^2$
[111]	$A_1 = \frac{9}{8} \frac{\rho_o}{C_{11} + 2C_{12} + 4C_{44}} \left( 1 + \frac{2}{9} \frac{3C_{111} + 6C_{112} + 3C_{144} + 6C_{166} + C_{123} + 2C_{456}}{C_{11} + 2C_{12} + 4C_{44}} \right) A_o^2$
[110]	$A_1 = \frac{3}{4} \frac{\rho_o}{C_{11} + C_{12} + 2C_{44}} \left( 1 + \frac{C_{111} + C_{112} + C_{166}}{C_{11} + C_{12} + 2C_{44}} \right) A_o^2$
Terms in $\omega$	
[001]	None
[111]	None
[110]	None

Table II. Harmonic amplitude and third order elastic constants. Transverse waves with {110} type polarization.

Terms in $\omega^2 s$	
Propagation Direction	Results
[001]	$B_1 = 0$
[111]	$B_1 = \frac{\sqrt{2}}{96v_2^2} \frac{12C_{111} - 12C_{112} + 3C_{144} - 3C_{166} + 4C_{123} - C_{456}}{C_{11} - C_{12} + C_{44}} B_o^2$
[110]	$B_1 = 0$
Terms in $\omega$	
[001]	$A_2 = -\frac{1}{8v_2} \frac{C_{11}}{C_{11} - C_{44}} \left( 1 + \frac{C_{166}}{2C_{11}} \right) B_o^2$
[111]	$A_2 = -\frac{1}{24v_2} \frac{C_{11} + 2C_{12} + 4C_{44}}{C_{12} + C_{44}} \left( 1 + \frac{12C_{111} - 3C_{144} + 6C_{166} - 2C_{123} - C_{456}}{6(C_{11} + C_{12} + 2C_{44})} \right) B_o^2$
[110]	$A_2 = -\frac{1}{8v} \frac{C_{11} + C_{12} + 2C_{44}}{C_{11} + C_{12}} \left( 1 + \frac{C_{144} + C_{166} + C_{456}}{2(C_{11} + C_{12} + 2C_{44})} \right) B_o^2$

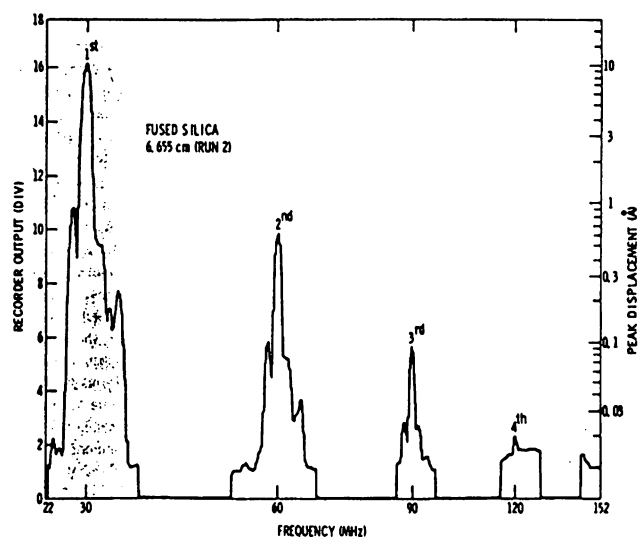


Figure 1 Multiple harmonics in fused silica using capacity microphone spectrometer.

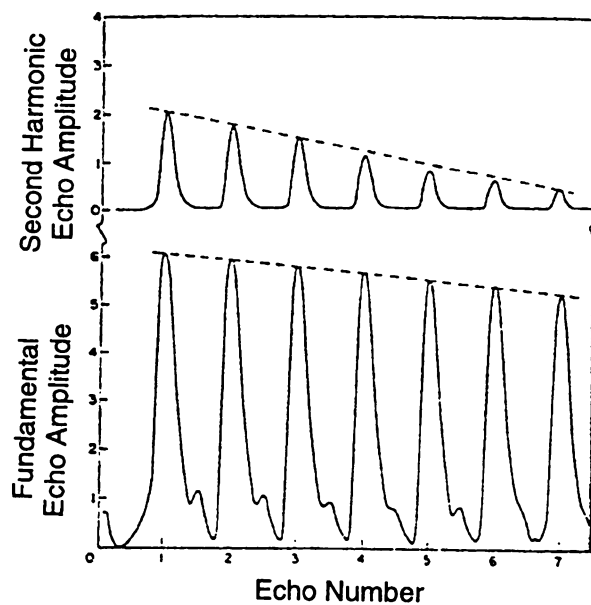


Figure 2 Logarithmic display of ultrasonic echoes in fused silica. Top trace is echo pattern of 2<sup>nd</sup> harmonic and bottom trace is the fundamental harmonic attenuation of 0.30 dB/cm and fundamental is 0.15 dB/cm.

research community in radiation damage research and the development of metallic work hardening models. Otto was deeply immersed in both.

The specific problem highlighted here was a study done to characterize details of point defect/dislocation interactions in copper single crystals.  $^{60}\text{Co}$   $\gamma$ -ray irradiation was used as a source for controlled defect production and internal friction measurements made at very small ( $\sim 2 \times 10^{-8}$ ) strain amplitudes were used for defect detection and defect/dislocation characterization. Major goals of the study were to determine the various thermodynamic activation energies that control defect diffusion in the sample and the behavior of the defect on the dislocation and, secondly, to determine the identity of the defect studied [18, 19, 20].

There was a large body of background material drawn upon in this work. First, a significant effort existed in the radiation damage community to identify specific defects that were mobile in various temperature ranges following irradiation with neutrons or other penetrating radiations. A major controversy existed as to the mobile defect in the temperature range covered in this work. (Stage III is essentially room temperature to approximately  $120^\circ\text{C}$ .) Arguments centered on whether the principal defect was a single vacancy or a single interstitial. A second body of knowledge that was used in the work was the recently developed and confirmed Granato-Lücke bowing string model of dislocation damping in which the measured internal friction and modulus defect were found to be extremely sensitive to defect pinning at low strain amplitudes ( $\sim 2 \times 10^{-8}$ ). In this work, internal friction measurements were used as “defect counters” during  $^{60}\text{Co}$   $\gamma$  irradiation at temperature. From these measurements, defect arrival at the dislocation lines via diffusive processes from their point of creation could be counted. References can be found in the cited literature.

A schematic representation of the model that Otto and his colleagues devised to characterize the defect/dislocation interaction at very low strain amplitudes and defect concentrations is shown in Fig. 3. They assumed that a  $\gamma$ -ray penetrates the crystal volume and creates a Frenkel pair of lattice defects via a Compton electron process. The edge of the cube is defined by the average dislocation length  $l_0$ . From their point of creation in the lattice, the defects, if they are mobile at the sample temperature, can diffuse to the dislocation and pin it. However, they can still diffuse along the dislocation and possibly be trapped at the end nodal points (jogs, clusters of vacancies/interstitials, etc. The reader is referred to references cited in the original paper). In this model it is envisioned that the system is in thermodynamic equilibrium so that a reverse flow of the defects from the dislocations back to the lattice are possible.

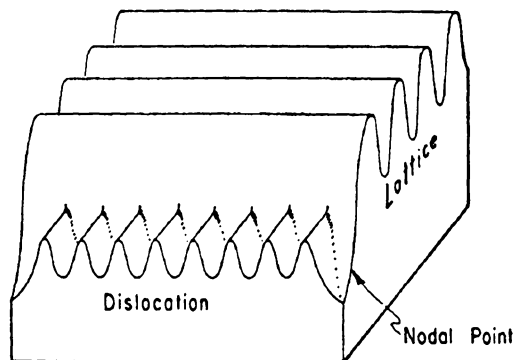


Figure 3 Schematic view of the model.

The model proposed above was summarized in a set of coupled equations as follows:

$$\frac{dn_L}{dt} = -\frac{n_L}{\tau_{LE}} + \tau_{DL}^{-1} \int_{-\frac{l_0}{2}}^{+\frac{l_0}{2}} \eta(x,t) dx + \phi, \quad (8a)$$

$$\frac{\partial \eta}{\partial t}(x,t) = D \frac{\partial^2 \eta(x,t)}{\partial x^2} + \frac{n_L}{l_0 \tau_{LE}} - \frac{\eta(x,t)}{\tau_{DL}}, \quad (8b)$$

$$\frac{dn_N}{dt} = -D \frac{\partial \eta(x,t)}{\partial x} \bigg|_{x=\pm \frac{l_0}{2}} = \frac{a_n}{\tau_{Du}} \bigg|_{x=\frac{l_0}{2}} - \frac{n_N}{\tau_{ND}}, \quad (8c)$$

and

$$2n_N + \int_{-\frac{l_0}{2}}^{+\frac{l_0}{2}} \eta(x,t) dx + n_L = \phi t \quad (8d)$$

in which

- $\tau_{LE}, \tau_{DL}, \tau_{DU}$ , and  $\tau_{ND}$  are, respectively, the relaxation times in an Arrhenius thermal activation relation for defect diffusion from lattice to the dislocation, emission from the dislocation back to the lattice, defect “pipeline” diffusion along the dislocation, and emission from the nodal point trap back to the dislocation.
- $D$  is the “pipeline” diffusion coefficient ( $= \frac{a^2}{2\tau_{Du}}$ ).
- $n_L, n_N$  are the numbers of defects in the lattice and in the nodal points.
- $\eta(x,t)$  is the linear concentration of defects on the dislocation segment.
- $n_D = \int_{-\frac{l_0}{2}}^{+\frac{l_0}{2}} \eta(x,t) dx$  is the number of pinning points.
- $\phi$  is the  $\gamma$  flux,  $t$  is time.

Thus Equation (8d) is a conservation equation that accounts for all defects produced.

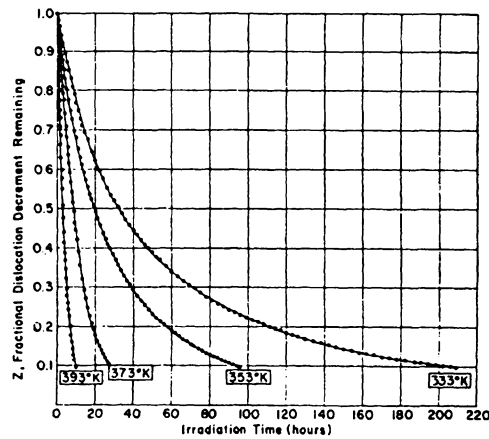


Figure 4 Fractional dislocation decrement remaining during irradiation at four different temperatures.



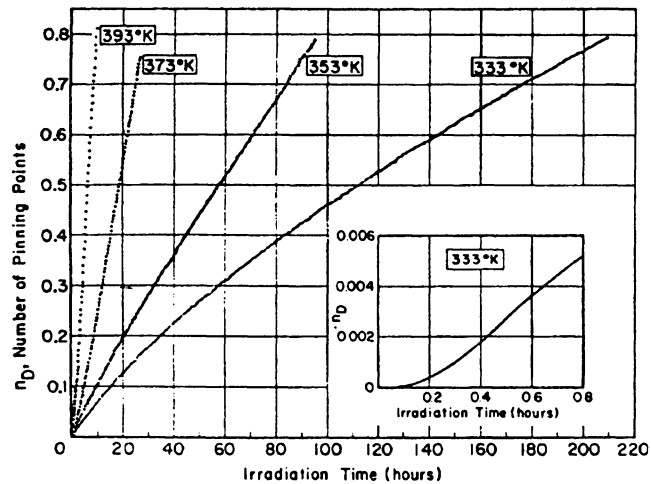


Figure 5 Pinning point accumulation as a function of irradiation time at four different temperatures.

Otto and his colleagues then proceeded to solve this set of equations for the four relaxation times in terms of known parameters and  $n_D$  the total number of defects (or pinning points) on a dislocation line of length  $l_o$ . As noted below,  $n_D$  is the observed number of pinning points derived from the measurements.

An example of the experimental results obtained that formed the basis for the analysis is given in Figs. 4 and 5. Figure 4 shows the fractional dislocation damping remaining as a function of irradiation time at temperature, and Fig. 5 shows the number of pinning points,  $n_D$ , added to the dislocation distribution, also as a function of irradiation time and temperature. Figure 5 was derived from Fig. 4 using the Granato-Lücke model for dislocation damping; the same results were obtained using elastic modulus results. The

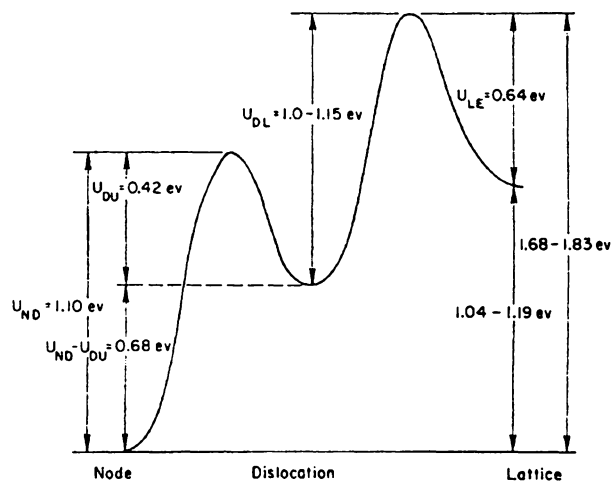


Figure 6 Schematic summary of the various energies.

Table III Energy values.

Relaxation Times	Energy (ev)	Description
$\tau_{ND}$	1.10	Escape energy from nodal trap to dislocation
$\tau_{Du}$	.42	"Pipeline" diffusion energy
--	.68	Binding energy to node
$\tau_{DL}$	1.0-1.15	Escape energy from dislocation to lattice
$\tau_{LE}$	0.64	Buck diffusion energy
--	0.36-0.51	Binding energy of defect to dislocation

parameter  $n_D$  is obviously the direct coupling parameter between the experimental work and the model given above.

With these results, a coherent picture of the defect dislocation at low defect concentrations was obtained. Figure 6 shows an "energy" level diagram that was developed to show schematically the diffusion and "bonding" of the defect to the dislocation, and Table III gives a summary of the energy specifics.

This study provided a number of significant results. First, it provided a complete and self-consistent picture of defect/dislocation interactions at small defect concentrations. Secondly, the work provided information regarding dislocation features such as jog energies and sizes. Finally, from the lattice diffusion energy obtained, 0.64 ev., it was concluded that the defect was a freely migrating interstitial. This value was in agreement with many other experiments of the times and helped to solidify this identification.

## SUMMARY

Otto's work was both broad in scope and deep in insight and rigor. As noted here, and in many other papers, he contributed significantly to technical advances in his time. He was both a great team player and an individual researcher who always provided an uplift when it was needed. I value both the professional relationship and personal friendship that I had with Otto and his family very deeply, and will miss him greatly.

## REFERENCES

1. A. Seeger and O. Buck, "Die Experimentelle Ermittlung der elastischen Konstanten höherer Ordnung", Z. f. Naturf., 15a, 1056 (1960).
2. W. Schüle, O. Buck, and E. Köster, "Eine Verformungsapparatur zur Messung des elektrischen Widerstands von Metallen bei tiefsten Temperaturen und Untersuchungen über das plastische Verhalten von Kupfereinkristallen", Z. f. Metallk., 53, 172 (1962).
3. O. Buck, "Verformung und elektrischer Widerstand von Kupfer-Einkristallen bei tiefsten Temperaturen", phys. stat. sol., 2, 535 (1962).
4. O. Buck and U. Essmann, "Deformation Twinning in Copper Single Crystals", in Deformation Twinning, Met. Soc. Conf., Vol. 25, Gordon and Breach, New York, London, 1964, p. 117.
5. O. Buck, "Mechanische Relaxation von Kupfer-Einkristallen", phys. stat. sol., 3, 1903 (1963).

6. O. Buck and U. Essmann, "Über die Bildung von Grosswinkelkorngrenzen während der Verformung von Metall-Einkristallen", *phys. stat. sol.*, 4, 143 (1964).
7. H. Kronmüller and O. Buck, "Zur Bestimmung der Domänenstruktur von Ni-Einkristallen aus Messungen der elektrischen Widerstandsänderung bei kleinen Magnetfeldstärken", *phys. stat. sol.*, 6, 207 (1964).
8. O. Buck and U. Essmann, "Die Bildung von Verformungszwillingen in Kupfer-Einkristallen", *Acta Met.*, 12, 1181 (1964).
9. O. Buck and D. O. Thompson, "Relation of Finite Amplitude Waves to Third Order Elastic Constants", *Mat. Sci. Eng.*, 1, 117 (1966).
10. J. Melngailis, A. A. Maradudin, and A. Seeger, *Phys. Rev.* 131 (1963), p. 1972.
11. A. L. Polykova, *Sov. Phys. Solid State* 6 (1964), p. 50.
12. A. A. Gedroits and V. A. Krasilnikov, *Sov. Phys. JETP*, 16 (1963), p. 1122.
13. M. A. Breazeale and D. O. Thompson, *Appl. Phys. Letters*, 3 (1963), p. 77.
14. F. R. Rollins, *Appl. Phys. Letters*, 2 (1963), p. 147.
15. J. H. Parker, E. F. Kelly, and D. J. Bolef, *Appl. Phys. Letters*, 5 (1964), p. 7.
16. D. O. Thompson, M. A. Tennison, and O. Buck, "Reflections of Harmonics Generated by Finite-Amplitude Waves", *J. Acoust. Soc. Am.*, 44, 435 (1968).
17. R. Bruce Thompson, O. Buck, and D. O. Thompson, "Higher Harmonics of Finite Amplitude Ultrasonic Waves in Solids", *J. Acoust. Soc. Am.*, 59, 1087 (1976).
18. D. O. Thompson, O. Buck, R. S. Barnes, and H. B. Huntington, "Diffusional Properties of the Stage III Defect in Copper. I. Experimental Results", *J. Appl. Phys.*, 38, 3051 (1967).
19. D. O. Thompson, O. Buck, H. G. Huntington, and R. S. Barnes, "Diffusional Properties of the Stage III Defect in Copper. II. A Model for Defect-Dislocation Interactions", *J. Appl. Phys.*, 38, 3057 (1967).
20. D. O. Thompson and O. Buck, "Diffusional Properties of the Stage III Defect in Copper. III. Bulk Diffusion", *J. Appl. Phys.*, 38, 3068 (1967).